Sua Pan Surface Bidirectional Reflectance: A Case Study to Evaluate the Effect of Atmospheric Correction on the Surface Products of the Multi-angle Imaging SpectroRadiometer (MISR) During SAFARI 2000

Wedad A. Abdou, Stuart H. Pilorz, Mark C. Helmlinger, James E. Conel, David J. Diner, *Member, IEEE*, Carol J. Bruegge, John V. Martonchik, *Member, IEEE*, Charles K. Gatebe, Michael D. King, *Senior Member, IEEE*, and Peter V. Hobbs

***Abstract*—This paper presents a validation case study of Multi-angle Imaging SpectroRadiometer (MISR) surface products where its bidirectional reflectance (BRF) measurements during the Southern Africa Regional Science Initiative (SAFARI 2000) campaign are compared with those coincidently evaluated on the ground and from the air, using the Portable Apparatus for Rapid Acquisition of Bidirectional Observations of Land and Atmosphere (PARABOLA) and Cloud Absorption Radiometer observations, respectively. The presence of haze and smoke during the campaign provided a case study to evaluate the effect of atmospheric correction on MISR surface products. Two surface types were considered in the analyses: the bright desert-like surface of the Pan and the dark grassland that surrounds it. The results show that for the dark surface the BRF values retrieved from MISR are in good agreement, within 5%, with those obtained from field data. For the bright desert-like pan surface, better agreement, within $\sim$10%, was found in all channels on the clear day but only in the forward scattering on the hazy day. A comparison of MISR aerosol retrievals to those obtained from three independent ground measurements suggests that, in the presence of a highly reflective surface, small uncertainties in the MISR aerosol retrievals become magnified at larger optical depths, causing errors in the surface BRF retrievals.**

***Index Terms*—Aerosols, bidirectional reflectance function (BRF), remote sensing, surface.**

Manuscript received October 29, 2004; revised February 6, 2006. This work was conducted at the Jet Propulsion Laboratory, California Institute of Technology, as part of the SAFARI 2000 Southern African Regional Science Initiative, under contract with the National Aeronautics and Space Administration (NASA). The University of Washington team was supported by NASA and the National Science Foundation.

W. A. Abdou is with the California Institute of Technology and the Earth Science Division, Jet Propulsion Laboratory, Pasadena, CA 91109 USA (e-mail: wedad.abdou@jpl.nasa.gov).

S. H. Pilorz, M. C. Helmlinger, J. E. Conel, D. J. Diner, C. J. Bruegge, and J. V. Martonchik are with the Jet Propulsion Laboratory, California Institute of Technology, Pasadena, CA 91109 USA.

C. K. Gatebe is with the Goddard Earth Sciences and Technology Center, University of Maryland, Baltimore County, Baltimore, MD 21228 USA.

M. D. King is with the Earth–Sun Exploration Division, NASA Goddard Space Flight Center, Greenbelt, MD 20771 USA.

P. V. Hobbs is with the Department of Atmospheric Sciences, University of Washington, Seattle, WA 98195 USA.

Digital Object Identifier 10.1109/TGRS.2006.876031

I. Introduction

THE Multi-angle Imaging SpectroRadiometer (MISR) was launched on December 18, 1999, into a 705-km sun-synchronous Earth orbit aboard the Earth Observing System (EOS) Terra spacecraft. The MISR instrument [1] has nine charge-coupled device (CCD) pushbroom cameras that view the Earth's surface in four spectral bands centered at 446, 558, 672, and 866 nm, and at angles of 0° (An), 26.1° (Af, Aa), 45.6° (Bf, Ba), 60.0° (Cf, Ca), and 70.5° (Df, Da), relative to nadir, in both forward (f) and aft (a) along the direction of flight, where the notations in parentheses are shorthand names for the cameras. The major science goal of EOS and of MISR is to provide well-calibrated and validated measurements of key parameters that are crucial to the long-term assessment of temporal variations in the Earth's radiation budget especially those due to clouds, aerosols, and land-surface albedo. The MISR data products provide information on atmospheric aerosol (e.g., optical depth, column-averaged particle size distribution, single-scattering albedo, etc.), the surface bidirectional reflectance factor (BRF), and the hemispherical directional reflectance factor (HDRF).[1]

The BRF, an inherent property of the surface that characterizes its directional reflectance anisotropy, is defined as the ratio of the radiance reflected by the target surface in a specific direction to that reflected in the same direction by a perfectly diffuse (Lambertian) surface illuminated by the same collimated beam (i.e., direct illumination only). The HDRF characterizes the angular reflectance properties of the surface under ambient illumination (i.e., in presence of diffuse illumination), hence its dependency on atmospheric conditions. The integration of the BRF and the HDRF over view angles provides the directional-hemispherical reflectance (DHR) and the bihemispherical reflectance (BHR). The latter is commonly known as the albedo, while the DHR is sometimes referred to as the black-sky albedo (i.e., the albedo in the special case of illumination from a collimated beam—detailed definitions of these surface parameters are given in [2] and [3].

[1]For more information on MISR mission and data products see http://www-misr.jpl.nasa.gov and http://eosweb.larc.nasa.gov/PRODOCS/misr/table_misr.html, respectively.

Proper knowledge of surface albedo is crucial to the understanding of the radiative processes that govern the Sun–Earth system and to the assessment of the Earth's radiation budget. It is, therefore, of interest to ensure accurate surface measurements from satellite instruments, such as MISR. This paper describes a validation case study of MISR surface products, specifically the BRF, by comparing their values as retrieved from MISR to those determined simultaneously, but independently, from other measurements. Because atmospheric correction is crucial to the MISR surface retrieval process, it is important to examine MISR aerosol products, mainly the aerosol optical depth and type, and their effects on the accuracy of the retrieved BRF.

The Southern Africa Regional Science Initiative (SAFARI 2000) dry season field study,[2] carried out in the year 2000 during August and September, provided an opportunity to perform this validation experiment. The presence of haze and smoke during the campaign made available a unique set of data that are valuable for the evaluation of MISR atmospheric correction process. A wide range of intensive ground- and airborne-based measurements of the surface and atmosphere properties were coordinated in that campaign during Terra overpasses [4], [5]. Several of these ground and aircraft measurements are employed in this study.

II. MISR Surface Retrieval Strategy

The MISR surface retrieval algorithm involves inversion of the radiative transfer equation [6] to convert the observed top-of-atmosphere (TOA) radiance (normalized to an Earth–Sun distance of 1 AU and corrected to ozone absorption) to surface parameters. This approach requires knowledge of the atmosphere's reflective and transmissive properties, both of which are functions of aerosol optical depth and type. These atmospheric characteristics are determined in the MISR aerosol retrieval process, based on a principal component analysis of the TOA radiance [7], [8]. The technique does not require knowledge of the absolute surface reflectance or its spectral characteristics but does require sufficient scene spatial contrast at various MISR view angles. An essential component of the aerosol retrieval process is a lookup table (LUT) of path radiances simulated for a preselected set of aerosol mixtures that are commonly found in the atmosphere. Once the atmospheric properties are determined, the strategy is to retrieve the surface HDRF first and then proceed to obtain the BRF. Determination of the HDRF involves removal of the effects of atmospheric path radiance and the upward direct and diffuse transmission effects on the surface reflected radiance. The surface BRF is then derived from the HDRF by removing the effects of downward diffuse sunlight and assuming a parameterized BRF [9]. The LUT is central to this atmospheric correction process and the selected aerosol mixtures greatly impact the accuracy of retrieving the aerosol and, consequently, the surface products. The BRF measurements at SAFARI 2000 present an opportunity to evaluate the effect of the above atmospheric correction on MISR surface retrieval. Details of MISR aerosol and surface retrieval algorithms are beyond the scope of this work and could be found in [8] and [10].

[2]http://daac.ornl.gov/S2K/safari.html

III. Surface BRF Measurements at SAFARI 2000

The SAFARI campaign covered multiple sites in Southern Africa. This work focuses only on the data collected at Sua Pan (20.6° S, 26.1° E), one of the salt pans in northeastern Botswana. The pan is about 3500 km^2 of bright desert-like surface surrounded by dark grasslands. Fig. 1 shows MISR image of the Sua Pan site from space on the clear day of August 27. The locations of the field campaign site and measurements are defined by the rectangular box and the "x" marks, respectively. The BRF retrieved from MISR data at these locations are compared with the coincident ground and airborne measurements. The three independent measurements cover: 1) the bright desert-like surface of the pan and 2) the dark dry grassland that surrounds the pan. Details of these measurements are described next.

A. MISR Measurements

Two MISR data sets obtained at Sua Pan, on August 27 and September 3, 2000, are selected for this study (it is important to note that the MISR data used here are the publicly available MISR surface and aerosol products version F04_0015 and F07_0015, respectively.) On these two days, at ~0852 UTC (~1052 local time), MISR passed over Sua Pan, in orbits 3684 (path 172, block 107) and 3786 (path 173, block 107), respectively. MISR viewing geometries on both days are listed in Tables I and II and, as expected in the Southern Hemisphere, MISR forward cameras were viewing the pan in the backscattering directions. The MISR images of Sua Pan indicate clear atmospheric conditions on August 27 and thick haze and smoke on September 3, due to wild and man-made grass fires that erupted earlier at several spots near the pan. This large difference in aerosol loading provides the opportunity to evaluate the effect of the MISR atmospheric correction process on retrieving the surface parameters. MISR BRF values, at each of the nine view angles, is averaged over a group of 2×2 (1.1 km) pixels that cover each ground locations.

B. Ground Measurements

The MISR validation team was present at Sua Pan from August 24 to September 4, 2000, and made daily measurements of the surface directional reflectance using the Portable Apparatus for Rapid Acquisition of Bidirectional Observations of Land and Atmosphere (PARABOLA) version III [11]. The third-generation sphere-scanning radiometer built by Sensit Corporation (Mayville, ND) represents a substantial revision in design and capability over the first version of this instrument [12].

PARABOLA III consists of two separate sensor heads mounted at opposite ends of a center-suspended horizontal scanning arm that rotates continuously through 360° about a vertical axis. Each sensor head contains the detector assemblies for four of eight channels (444, 551, 650, 860, 944, 1028, 1650, and 400–700 nm). Each individual head scans synchronously with the other from zenith to nadir in vertical angle. The combined synchronized motion of the heads about both axes generates a steppers pattern of 5° circular full apex angle overlapping fields of view of sky hemisphere, and a series of 5° ellipsoidal pixels on the ground that increase in length from nadir to horizon (~10 cm at nadir to ~10 m at ~80°, when the PARABOLA is set ~2 m above ground). An entire scan of both

Fig. 1. MISR image of Sua Pan, Botswana (20.6° S, 26.1° E), on the clear day of August 27. The image is an RGB composite from the nadir camera, at 275-m resolution. The rectangular box shown in this figure defines the ground campaign site. The "X" marks the locations of the ground and airborne measurements used in the analyses. MISR image of Sua Pan on September 3 (not shown here) shows heavy haze due to smoke from biomass fires that were present near Sua Pan.

TABLE I
MISR ZENITH AND AZIMUTH (RELATIVE TO THE SUN) VIEW ANGLES ON AUGUST 27, 2000. AT OVERPASS TIME THE SUN ZENITH ANGLE WAS 37.85°

Camera	Df	Cf	Bf	Af	An	Aa	Ba	Ca	Da
Zenith angles	70.6	60.5	46.1	26.7	3.6	26.0	45.4	59.9	70.3
Relative Azimuth	159.3	159.9	161.1	164.6	119.1	30.3	26.7	25.5	25.0
Scattering Angles	141.1	150.7	163.5	168.6	146.6	121.3	102.1	87.9	77.7

TABLE II
MISR ZENITH AND AZIMUTH (RELATIVE TO THE SUN) VIEW ANGLES ON SEPTEMBER 3, 2000. AT OVERPASS TIME THE SUN ZENITH ANGLE WAS 34.6°

Camera	Df	Cf	Bf	Af	An	Aa	Ba	Ca	Da
Zenith angles	70.4	60.3	46.1	27.4	10.4	28.1	46.5	60.5	70.8
Relative Azimuth	152.6	150.5	146.5	136.0	64.5	2.65	12.7	16.7	19.0
Scattering Angles	138.9	147.1	155.9	156.5	139.6	116.9	99.1	85.7	75.9

sky and ground hemispheres generates $2664\ (=37 \times 72)$ pixels in about 3 min including downloading to memory. A Spectralon panel, placed in the southwest corner of the PARABOLA nadir field of view, provides the perfect Lambertian standard reference required for the BRF calculations (based on the definition given in the introduction). In practice, the Spectralon reflectance deviates slightly from that of a perfect Lambertian surface and a correction factor, equal to the Spectralon BRF at the specific viewing and illuminating geometry, is required to correct for the imperfect Lambertian properties. A database for the Spectralon BRF is available from Bruegge *et al.* [13] to determine the required correction factor. Details of the PARABOLA III measurements and calibration procedures are described in [11].

The surface BRF is retrieved from the PARABOLA data using a methodology developed by Martonchik [14]. The tech-

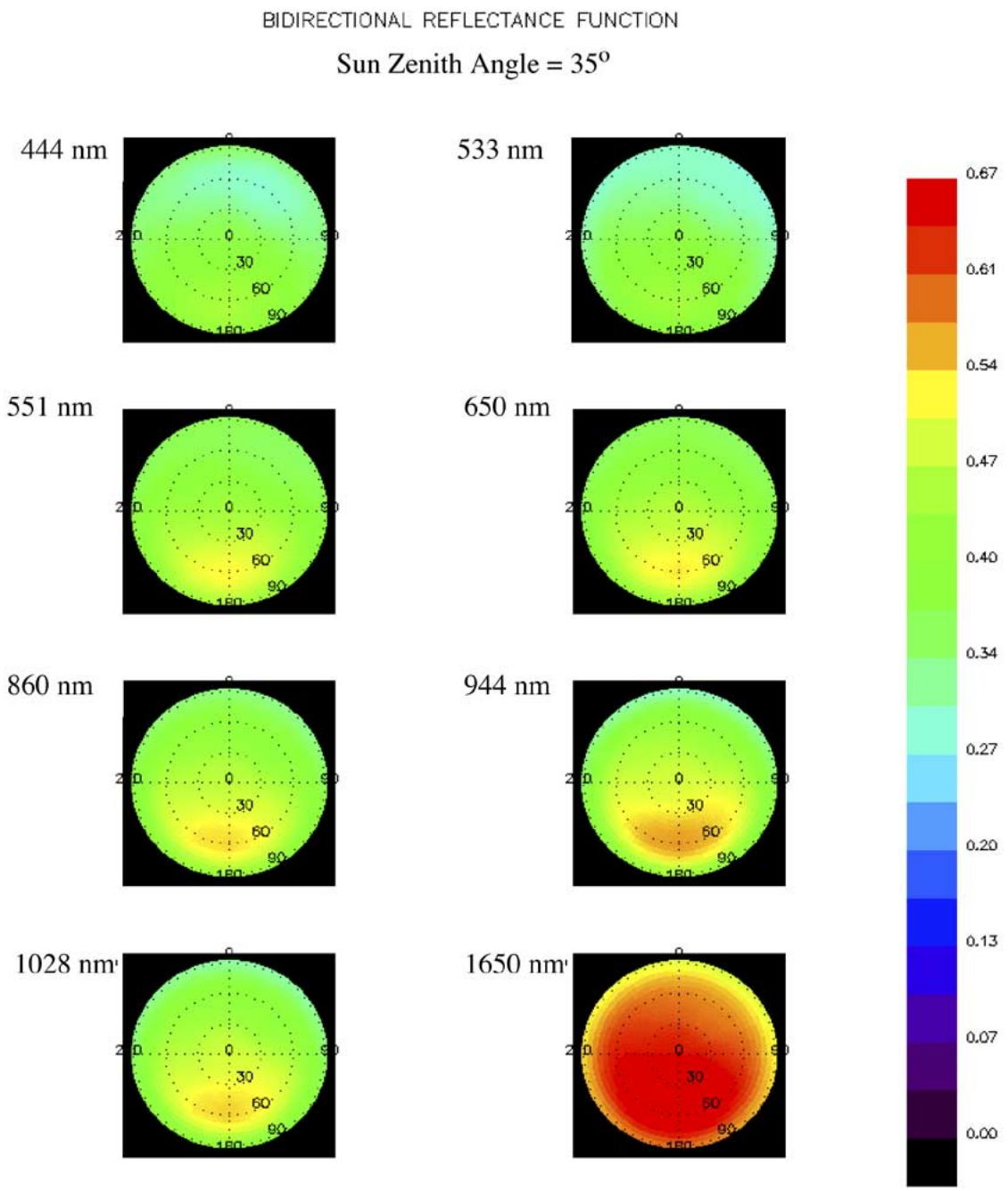

Fig. 2. Polar plot of the surface BRF retrieved from the PARABOLA measurements at the bright-desert like surface of Sua Pan on August 27, 2000, during a Terra overpass. The sun zenith angle for the data in this plot is $\sim 35°$.

nique requires measurements, at the same location, over a range of solar angles, preferably from sunrise to noon or from noon to sunset. The data obtained during the clear day of August 27 and the hazy day of September 3 were processed, as described by Abdou *et al.* [15] and examples of the BRF retrieved from the PARABOLA data on August 27 are illustrated in Fig. 2. This polar plot shows an almost diffusely reflecting surface, that exhibit no strong angular signatures. The surface BRF increases with wavelengths and is enhanced in the backscattering directions.

For meaningful comparison with MISR, the PARABOLA data must represent the reflectance over an area equal in size to that covered by MISR footprints (1.1×1.1 km). To make sure of that, a portable spectrometer was used to evaluate the average reflectance of the pan surface within this area. The portable spectrometer, manufactured by Analytical Spectral Devices, Incorporated (ASD) (Boulder, CO), provides rapid estimates of the surface spectral HDRF (in the nadir direction) between 350 and 2500 nm at an average spectral resolution of $\sim$10 nm. With a field of view of 8°, the hand-held spectrometer has a footprint of $\sim$15 cm. The ASD sampling technique is to alternately measure the radiance reflected from the target surface and that reflected from a reference Lambertian surface, in this case the Spectralon panel and the surface HDRF is determined by the ratio of the two radiances. The correction factor, mentioned above, is applied to account for the devia-

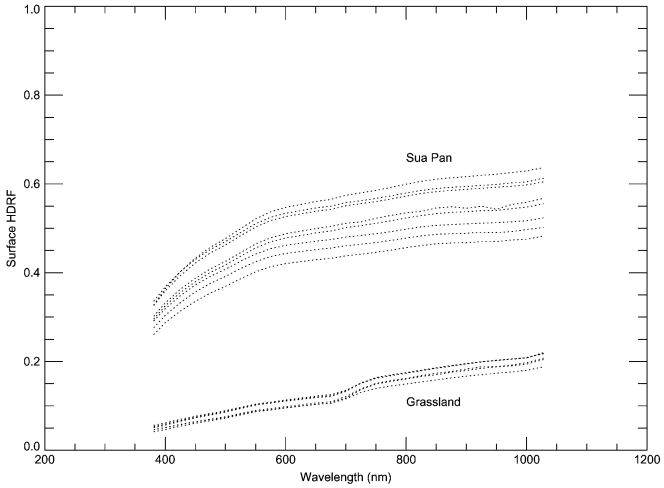

Fig. 3. Surface HDRF as measured by the ASD instrument on August 27 and September 3 at various locations on the pan surface and on the grassland, within the box shown in Fig. 1. The ASD data represent the range of brightness of the pan surface and of the grassland.

tion of the Spectralon reflectance from Lambertian. The ASD measurements were made at 20 points along representative transects laid out over the area surrounding the PARABOLA location. The few seconds sampling time allowed numerous ground spectra to be made without significant changes in the illumination or atmospheric conditions during the Terra overpass time. The ASD data were collected at various locations on the pan and on the grassland (within the rectangle shown in Fig. 1) on August 24, 25, 27, and 30, 2000 and on September 3, 2000, under cloud-free conditions and close to the Terra satellite overpass times. Fig. 3 illustrates the range of these measurements. The ASD data obtained at various points within the footprint of the MISR 2×2 pixels were averaged and were used to normalize the PARABOLA BRF in the nadir. A global positioning system (GPS) was used to geolocate the ground field measurements to help minimize errors in collocating various data. The PARABOLA provides the BRF within ~ 2 to 3% accuracy at solar and view angles smaller than $\sim 45^\circ$ and within $\sim 8\%$ at more oblique angles [15]. In the present analyses, an upper limit of 10% uncertainty is assumed.[3]

C. Airborne Measurements

BRF measurements were made during the MISR overpass with the Cloud Absorption Radiometer (CAR) that flew aboard the University of Washington Convair-580 research aircraft over Sua Pan on September 3 [16]. The CAR is an airborne multi spectral scanning radiometer developed at Goddard Space Flight Center originally for the study of spectral cloud absorption [17]. The instrument is designed to scan the sky downwelling and the ground upwelling radiances from zenith to nadir in 1° field of view in 14 spectral channels (340–2300 nm). Under cloud-free conditions, the multiangle viewing geometry of the CAR allows determination of the directional reflectance properties of terrestrial surfaces [18]–[20]. As the Convair-580 flew in ~ 3 km circles at 600-m altitude above the Sua Pan, the CAR made several complete orbital measurements that extended from 0949 to 1000 UTC at a solar zenith angle of $\sim 28.5^\circ$. At 600-m altitude, the resolution of the CAR is ~ 10 m at nadir and ~ 270 m at 80° view angle. The surface BRF was retrieved, with better than 5% accuracy, from the CAR measurements after applying an atmospheric correction to remove the radiances scattered by the ambient atmosphere [16].

[3]For more on the measurements, see field engineers reports at http://www-misr.jpl.nasa.gov/mission/valwork/val_reports/000813_safari/safari.html.

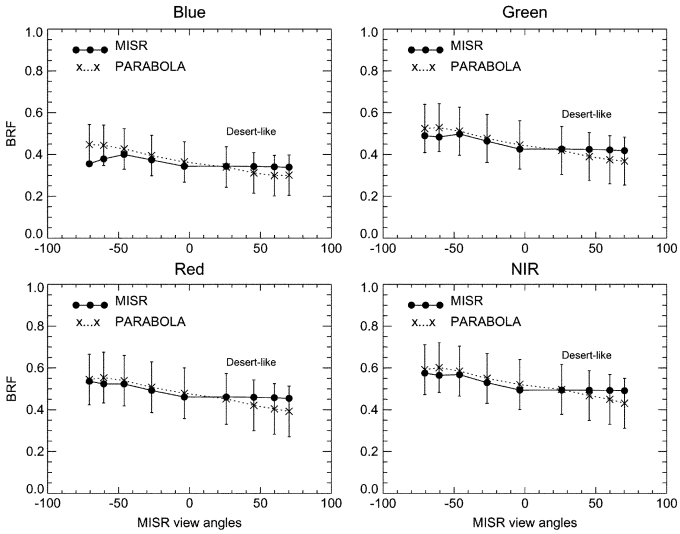

Fig. 4. Comparison of the BRF retrieved from MISR data at pan surface on August 27 with those retrieved on the same day from the ground-based PARABOLA at MISR four wavelengths. The error bars represent the estimated maximum error (10%) in ground measurements.

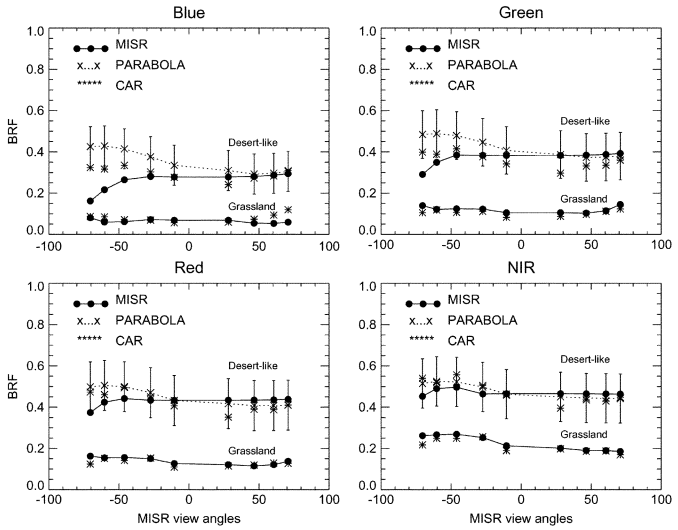

Fig. 5. Comparison of the BRF retrieved from MISR data at Sua Pan on September 3, with those retrieved from the ground-based PARABOLA and the aircraft-based CAR data. No PARABOLA data were available at the grassland. The error bars are the estimated maximum error (10%) in ground measurements.

IV. Results

The PARABOLA and CAR BRFs were linearly interpolated to MISR viewing geometries (Tables I and II) and wavelengths and compared with the values retrieved from MISR data on August 27 and September 3, as shown in Figs. 4 and 5, respectively. There were no PARABOLA data available for the grassland on either days and no CAR data available on August 27. The data

were collocated at the two sites (marked with "X" in Fig. 1) that characterize the bright desert-like surface of the pan and the dry grassland that surrounds it. The CAR data were obtained on September 3 about one hour after the Terra overpass and were corrected for the change in the solar angle (by multiplying by a factor equal to the ratio of the cosines of the two solar angles).

Fig. 4 shows that on the clear day of August 27, the BRFs retrieved from MISR data for the bright desert-like surface agree within 0.01 to 0.05, in absolute value, with the ground-based BRF in all of the channels except in the two blue backscattering channels, at 70.6° and 60.5°, where the agreement is ~ 0.1. In the nadir and near nadir channels, the agreements between MISR and the PARABOLA measurements are within < 0.025. MISR accuracy requirements for the BRF retrievals are the largest of $+0.03$ or 10%. However, the differences shown in Fig. 4 between MISR and ground-based BRF values, for all the channels, are within the standard deviation of the ASD data at the pan surface (see Fig. 3).

Fig. 5 illustrates the data collected on the hazy day of September 3. On that day, CAR data were available for the bright desert and grassland surface types. For the bright desert-like surface of the pan, MISR BRF values retrieved in the forward scattering channels agree within 0.01 to 0.05, in absolute values, with the corresponding airborne and ground measurements. In the backscattering direction, however, MISR BRFs are underestimated relative to the CAR and PARABOLA data with maximum disagreement in the most oblique cameras. Fig. 5 also illustrates the comparison between the BRF values retrieved on the same day from MISR and the CAR instrument at the dark grassland site. The agreements in this case are mostly within 0.01.

V. Discussion and Conclusion

The above results show that MISR BRFs are mostly in reasonable agreements with the ground and airborne field measurements, except for the bright surface on the hazy day. This suggests the atmospheric correction process as one likely source of the discrepancy. The excellent agreement between MISR's and CAR's BRF values for the dark grassland site on the same hazy day appears inconsistent with this conclusion. The two other known sources of errors are MISR radiometric calibration and colocating and scaling the data. The first, validated to be within $\sim 4\%$ [21] for all spectral bands, does not explain errors in only some of the cameras. Also, using the numerous ASD data at various locations on the pan, and the field GPS data that accompanied the ground and aircraft measurements, and with a georegistration of MISR images better than one pixel [22], the colocation and scaling of the data were straightforward. This leaves the atmospheric correction process to be the most plausible source of the discrepancy shown in Fig. 5. To evaluate the effect of this process, MISR aerosol products are examined and compared with some of those made in the field on the ground and from the Convair-580.

A. Aerosol Field Measurements

The MISR team made several field measurements of the aerosol optical depth using auto tracking Reagan sun-radiometers. Two of these radiometers were used to measure the incident solar irradiance in ten spectral channels in the range 380–1030 nm. These instruments were calibrated (zero airmass instrument response determined) using the well-known Langley technique [23]. The Rayleigh scattering optical depth, required by this technique, is calculated from field measurements of atmospheric pressure. The residual optical depth consisting of the total instantaneous optical depth minus Rayleigh component is the starting point for simultaneous retrieval of the aerosol and ozone components using the procedure developed by Flittner *et al.* [24]. The average aerosol optical depth obtained from the sun photometers' measurements on August 27 and September 3 are illustrated in Fig. 6. The data on September 3 indicate the thick haze and smoke that were present on that day. The CIMEL Sunphotometer (manufactured by CIMEL Electronique, France) was also used to measure light scattering in the solar aureole, as well as in the almucantar and the principal plane. The CIMEL data provide the atmospheric optical depth, shown also in Fig. 6, but they are used, in addition, to determine the aerosol phase function, single-scattering albedo, and particle size distribution using the retrieval algorithm described by Dubovik and King [25]. The retrieved volume particle size distribution, shown in Fig. 7(a), has three modes with characteristic radii of about 0.1, 1.0, and 6.0 μm. No results were available for August 27, but those available on August 28 show a size distribution similar to the one obtained for September 3. The CIMEL results obtained for the SAFARI campaign sites are posted on the Aerosol Robotic Network (AERONET) website at aeronet.gsfc.nasa.gov [26].

Additionally, an integrating three-wavelength nephelometer and a Particle Measurement System (PMS) model PCASP-100X were aboard the Convair-580 to measure the vertical profiles of the aerosol light scattering coefficient and particle size distribution over Sua Pan on September 3 [27]. Fig. 7(b) compares the *in situ* particle size distribution with

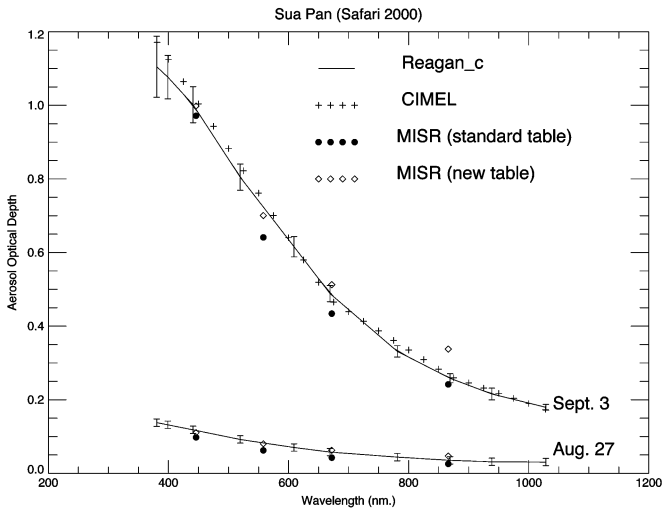

Fig. 6. Optical depth values measured by the sun-radiometers at Sua Pan, on August 27 and September 3, during the Terra overpass. Also shown, for comparison, are the corresponding optical depth values retrieved from MISR data using the standard LUT, containing 24 aerosol models (mixtures file version F03-0006) as well as those retrieved using a new LUT that contains 74 aerosol models.

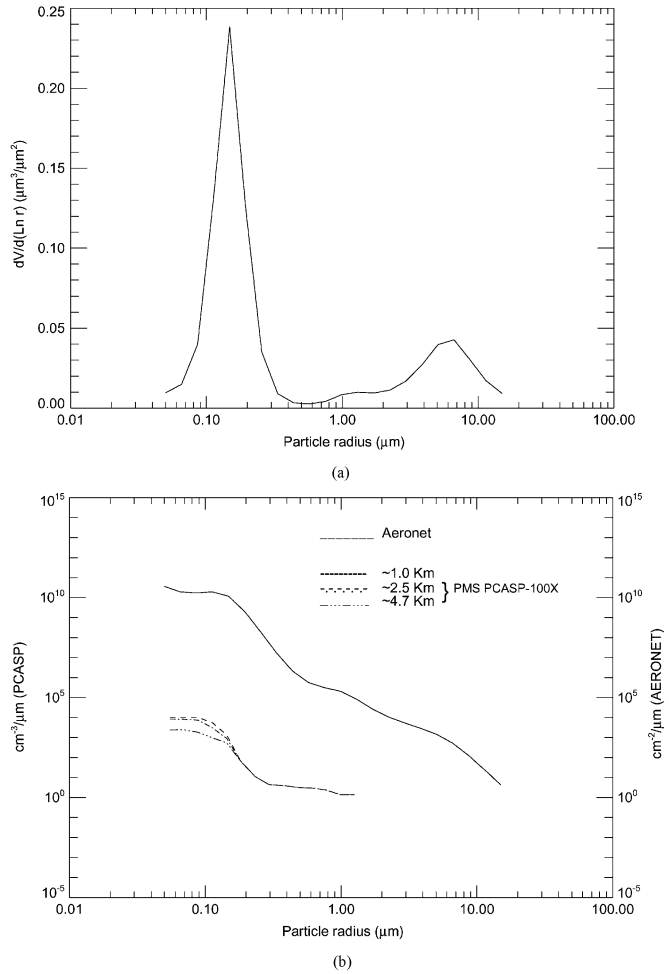

Fig. 7. (a) Aerosol column particle volume size distribution retrieved (using the Dubovik and King method [25]) from the CIMEL (AERONET) data at Sua Pan on September 3 and (b) the *in situ* particle size distribution in (left) units per cubic centimeter per micron measured at three different altitudes by the PMS PCASP-100X aboard the Convair-580. Also shown, for comparison, the aerosol column number density particle size distribution (right) in units per square centimeter per micron that is estimated from the data shown in (a) using an aerosol column length of 3 km.

that inverted from the CIMEL ground measurements [shown in Fig. 7(a)] after converting the latter to column number density particle size distribution (using an aerosol column length of $\sim$3 km). The *in situ* particle size distribution measurements indicate a well-mixed aerosol with at least two modes, one at $\sim$0.1 μm and the other at $\sim$1.0 μm radius. It should be noted that the *in situ* measurements are sensitive only to particle size in the range 0.06–1.5 μm in radius, while the AERONET inversion is sensitive to particles size from 0.05–15 μm. Within these radii range of overlapping sensitivity, the two independent field measurements, shown in Fig. 7(b), are reasonably consistent. Also, the vertical profiles of the aerosol light scattering coefficient was found consistent with that estimated from the AERONET data.

B. MISR Aerosol Measurements

The MISR aerosol retrievals over Sua Pan for August 27 and September 3 are shown in Fig. 6. The optical depth values retrieved on both days are underestimated relative to those retrieved in the field. Currently, the standard operational algorithm is based on a set of 24 aerosol models (mixture file version F03_0006) based on 11 pure particles (file version F04_0005 [28]. The retrieved aerosol model is a mixture of a small white particle (characteristic radius $= 0.06$ μ) with soot (characteristic radius of 0.012 μ). The mixture model has an effective single-scattering albedo of 0.88, in MISR green band, and an Angstrom coefficient of 2.1. This model is much smaller than, but as absorbing as, that retrieved from the airborne and ground measurements.

By examining the retrieved phase functions in the scattering angle range covered by MISR viewing geometries (Tables I and II), especially for the most oblique aft viewing, they were found to be larger than those corresponding to the particles retrieved from the field measurements. As a result, MISR retrieval process estimates more radiances than it actually observes and it compensates for the excess radiances by retrieving smaller optical depths and/or smaller surface BRF. This is most profound in the case of the hazy atmosphere over the bright pan surface, as shown in Fig. 5, due to the enhancement of the multiple scattering process in the presence of the highly reflective surface of the pan. The contribution of this process to the TOA radiance is the most dominant. The same uncertainties in the aerosol retrievals have insignificant effects on the BRFs retrieved at the dark grassland, where the multiple scattering process is impeded by the highly absorbing surface, or at the bright pan surface when the atmosphere is optically thin, such as on August 27, where the TOA radiances are dominated mostly by the light scattered directly from the surface.

It is clear from this and several other independent studies, that the aerosol models, preselected for MISR retrieval process, and the LUT containing the corresponding simulated radiances require improvement. A new table, that is now being introduced for operational retrievals, contains radiances simulated for 74 aerosol mixtures that are based on 21 pure particles. With this table, the retrieved optical depths, as shown in Fig. 6, are now closer to the field measurements. The retrieved aerosol models were mixtures, with various percentage by optical depth, of two particles with characteristic radii of 0.12 and 1.0 μm and single-scattering albedos of 0.9 and 1.0, respectively. These mixtures are closer in size to, but less absorbing than, the model retrieved from the field measurements. The new table has improved the retrieved aerosol optical depths but overestimated its single-scattering albedo and, most importantly, without significant changes in the BRF retrievals.

In conclusion, it is evident from these results that, in the case of bright surfaces under optically thick atmospheric conditions, the multiple scattering between aerosol particles and aerosol and surface, enhance the effect of any uncertainties in the aerosol properties causing significant errors in the surface BRF retrieval. Further work to isolate and evaluate more of these cases will be most valuable. Also, it is important to repeat this work for cases that involve heterogeneous surfaces and various degrees of brightness.

ACKNOWLEDGMENT

The authors thank B. N. Holben for making the CIMEL data available on the AERONET site.

REFERENCES

[1] D. J. Diner, J. C. Beckert, T. H. Reilly, C. J. Bruegge, J. E. Conel, R. A. Kahn, J. V. Martonchik, T. P. Ackerman, R. Davies, S. A. W. Gerstl, H. R. Gordon, J.-P. Muller, R. B. Myneni, P. J. Sellers, B. Pinty, and M.M. Verstraete, "Multi-angle Imaging SpectroRadiometer (MISR) instrument description and experiment overview," *IEEE Trans. Geosci. Remote Sens.*, vol. 36, no. 4, pp. 1072–1087, Jul. 1998.

[2] J. V. Martonchik, C. J. Bruegge, and A. H. Strahler, "A review of reflectance nomenclature used in remote sensing," *Remote Sens. Rev.*, vol. 19, pp. 9–20, 2000.

[3] F. E. Nicodemus, J. C. Richmond, J. J. Hsia, I. W. Ginsberg, and T. Limperis, "Geometric considerations and nomenclature for reflectance, U.S.A. Department of Commerce/National Bureau of Standards," *NBS Monogr.*, vol. 160, pp. 1–52, 1977.

[4] R. J. Swap, H. J. Annegarn, J. T. Suttles, J. Haywood, M. C. Helmlinger, C. Hely, P. V. Hobbs, B. N. Holben, J. Ji, M. D. King, T. Landmann, W. Maenhaut, L. Otter, B. Pak, S. J. Piketh, S. Platnick, J. Privette, D. Roy, A. M. Thompson, D. Ward, and R. Yokelson, "The Southern African Regional Science Initiative (SAFARI 2000): Overview of the dry-season field campaign," *South Afri. J. Sci.*, vol. 98, pp. 125–130, 2002.

[5] M. D. King, S. Platnick, C. C. Moeller, H. E. Revercomb, and D. A. Chu, "Remote sensing of smoke, land and clouds from the NASA ER-2 during SAFARI 2000," *J. Geophys. Res.*, vol. 108, p. 8502, 2003. DOI: 10.1029/2002JD003207.

[6] S. Chandrasekhar, *Radiative Transfer*. New York: Dover, 1960.

[7] J. V. Martonchik, D. J. Diner, K. A. Crean, and M. A. Bull, "Regional aerosol retrieval results from MISR," *IEEE Trans. Geosci. Remote Sens.*, vol. 40, no. 7, pp. 1520–1531, Jul. 2002.

[8] J. V. Martonchik, D. J. Diner, R. Kahn, M. M. Verstrate, B. Pinty, H. R. Gordon, and T. P. Ackerman, "Techniques for the retrieval of aerosol properties over land and ocean using multiangle imaging," *IEEE Trans. Geosci. Remote Sens.*, vol. 36, no. 4, pp. 1212–1227, Jul. 1998.

[9] H. Rahman, B. Pinty, and M. M. Verstraete, "Coupled surface-atmosphere reflectance (CSAR) model 2. Semiempirical surface model usable with NOAA Advanced Very High Resolution Radiometer data," *J. Geophys., Res.*, vol. 98, pp. 20 791–20 801, 1993.

[10] J. V. Martonchik, D. J. Diner, B. Pinty, M. M. Verstrate, R. B. Myneni, Y. Knyazikhin, and H. R. Gordon, "Determination of land and ocean reflective, radiative, and biophysical properties using multiangle imaging," *IEEE Trans. Geosci. Remote Sens.*, vol. 36, no. 4, pp. 1266–1281, Jul. 1998.

[11] C. J. Bruegge, M. C. Helmlinger, J. E. Conel, B. J. Gaitley, and W. A. Abdou, "PARABOLA III: A sphere-scanning radiometer for field determination of surface anisotropic reflectance functions," *Remote Sens. Rev.*, vol. 19, pp. 75–94, 2000.

[12] D. W. Deering and P. Leone, "A sphere-scanning radiometer for rapid directional measurements of sky and ground radiance," *Remote Sens. Environ.*, vol. 19, pp. 1–24, 1986.

[13] C. J. Bruegge, N. L. Chrine, and D. Haner, "A Spectralon BRF data base for MISR calibration applications," *Remote Sens. Environ.*, vol. 76, pp. 354–366, 2001.

[14] J. V. Martonchik, "Retrieval of surface directional reflectance properties using ground level multiangle measurements," *Remote Sens. Environ.*, vol. 50, pp. 303–316, 1994.

[15] W. A. Abdou, M. C. Helmlinger, J. E. Conel, C. J. Bruegge, S. H. Pilorz, J. V. Martonchik, and B. J. Gaitley, "Ground measurements of surface BRF and HDRF using PARABOLA III," *J. Geophys. Res.*, vol. 106, pp. 11 967–11 976, 2000.

[16] C. K. Gatebe, M. D. King, S. Platnick, G. T. Arnold, E. F. Vermote, and B. Schmid, "Airborne spectral measurements of surface-atmosphere anisotropy for several surface and ecosystem over Southern Africa," *J. Geophy. Res.*, vol. 108, no. D13, p. 8489, 2003. DOI: 10.1029/2002JD002397.

[17] M. D. King, M. G. Strange, P. Leone, and L. R. Blaine, "Multiwavelength scanning radiometer for airborne measurements of scattered radiation within clouds," *J. Atmos. Oceanic Technol.*, vol. 3, pp. 513–522, 1986.

[18] C. K. Gatebe, M. D. King, S. C. Tsay, Q. Ji, G. T. Arnold, and J. Y. Li, "Sensitivity of off-nadir zenith angles to correlation between visible and near-infrared reflectance for use in remote sensing of aerosol over land," *IEEE Trans. Geosci. Remote Sens.*, vol. 39, no. 4, pp. 805–819, Apr. 2001.

[19] P. F. Soulen, M. D. King, S. C. Tsay, G. T. Arnold, and J. Y. Li, "Airborne spectral measurements of surface anisotropy during the SCAR-A, Kuwait oil fire, and TARFOX experiment," *J. Geophys. Res.*, vol. 105, pp. 10 203–10 218, 2000.

[20] S. C. Tsay, M. D. King, G. T. Arnold, and J. Y. Li, "Airborne spectral measurements of surface anisotropy during SCAR-B," *J. Geophys. Res.*, vol. 103, pp. 31 943–31 954, 1998.

[21] C. J. Bruegge, N. L. Chrine, R. R. Ando, D. J. Diner, W. A. Abdou, M. C. Helmlinger, S. H. Pilorz, and K. Thome, "Early validation of the Multi-angle Imaging SpectroRadiometer (MISR) radiometric scale," *IEEE Trans. Geosci. Remote Sens.*, vol. 40, no. 7, pp. 1477–1492, Jul. 2002.

[22] V. Jovanovic, M. M. Smyth, J. Zong, R. Ando, and G. W. Bothwell, "MISR in-flight camera geometric model Calibration and georectification performance," *IEEE Trans. Geosci. Remote Sens.*, vol. 40, no. 7, pp. 1512–1519, Jul. 2002.

[23] G. E. Shaw, J. A. Reagan, and B. M. Herman, "Investigations of atmospheric extinction using direct solar radiation measurements made with a multiple wavelength radiometer," *J. Appl. Meteorol.*, vol. 12, pp. 374–380, 1973.

[24] D. E. Flittner, B. M. Herman, K. J. Thome, and J. M. Simpson, "Total ozone and aerosol optical depths inferred from radiometric measurements in the Chappuis absorption band," *J. Atmos. Sci.*, vol. 50, no. 8, pp. 1113–1121, 1993.

[25] O. Dubovik and M. D. King, "A flexible inversion algorithm for retrieval of aerosol optical properties from sun and sky radiance measurements," *J. Geophys. Res.*, vol. 105, pp. 20 673–20 696, 2000.

[26] B. N. Holben, T. F. Eck, I. Slutsker, D. Tanre, J. P. Buis, A. Setzer, E. Vermote, J. A. Reagan, Y. Kaufman, T. Nakajima, F. Lavenu, I. Jankowiak, and A. Smirnov, "AERONET—A federal instrument network and data archive for aerosol characterization," *Remote Sens. Environ.*, vol. 66, pp. 1–16, 1998.

[27] P. V. Hobbs, "Technical appendix: An overview of the university of Washington's airborne measurements in the SAFARI 2000 field study in Southern Africa," *J. Geophys. Res.*, vol. 108, no. D13, p. 8487, 2003. DOI: 10.1029/2002JD002325.

[28] R. A. Kahn, B. J. Gaitley, J. V. Martonchik, D. J. Diner, K. A. Crean, and B. Holben, "MISR global aerosol optical depth validation based on two years of coincident AERONET observations," *J. Geophys. Res.*, vol. 110, no. D10, D10s04, 2005. DOI: 10.1029/2004JD004706.

Author photographs and biographies not available at the time of publication.